NUMERICAL SIMULATION OF CHEMICALLY INDUCED PERMEABILITY CHANGES DURING HEAT MINING IN HOT AQUIFERS

M. KÜHN[1], W. SCHNEIDER[1], J. BARTELS[2], H. PAPE[3] & C. CLAUSER[4]

[1]Wasserwirtschaft und Wasserversorgung, TUHH, Hamburg, Germany
[2]LUNG, Mecklenburg-Vorpommern, Schwerin, Germany
[3]Geodynamik, Rheinische Friedrich-Wilhelms Universität, Bonn, Germany
[4]Geowissenschaftliche Gemeinschaftsaufgaben, Hannover, Germany

SUMMARY - SHEMAT is a new finite difference code for simulating hydro-geothermal reservoirs. Flow, heat transfer, transport of dissolved substances, and geochemical reactions are mutually coupled. Dissolution and precipitation of matrix minerals are calculated by an extended version of the geochemical modeling code PHRQPITZ (Plummer et al., **1988).** Chemical water-rock interactions change the porosity which influences flow and transport properties of the reservoir. In SHEMAT this is taken into account by a fractal model of the pore space structure. A case study of the injection well of a geothermal installation has been carried out, focussing on the near vicinity of the borehole. The injection of cool water exerts a great influence on the hydraulic conductivity of the aquifer indicating continuous head pressure increase at the well. Dissolution and precipitation of anhydrite induced by the temperature changes increase the permeability of the formation in a growing region around the borehole and decrease it at the temperature front. In the initial period of aquifer exploitation considered here the negative effect of the cold water on the injectivity is partially compensated by the relocation of anhydrite.

1. INTRODUCTION

Due to geological circumstances the exploitation of hydro-geothermal energy in Germany for space and district heating is mainly provided from deep sandstone aquifers. The common arrangement of boreholes is the doublet, consisting of one well for hot water production and one well for cool water reinjection. One reason for water injection is to maintain the reservoir pressure, but the more important reason is to avoid contamination of aquifers near the surface by the geothermal brines.

Prerequisites for the formation properties are temperatures as high as possible and sufficiently large flow rates. Therefore depth and permeability are the key parameters for reservoir performance. During the reinjection of water into geothermal reservoirs it has been observed, that the injectivity of a well decreases as a result of formation damage. The problems culminate in an increase of pressure at constant flow rate, while the productivity remains unchanged. The practical consequences are a limitation of the flow rate, and a reduced operation period or a low viability of the geothermal plant. The major processes known to cause formation damage during reinjection are:

- plugging of pore throats by fines introduced in the formation by the injected water, or by fines which are eroded by the injected water (Vernoux and Ochi, **1994;** Kühn et al., **1998);**
- blocking of pore throats by gas bubbles formed due to degassing of the injected water (Boisdet et al., **1989);**
- precipitation of dissolved solids due to the mixing of injected water and formation water or due to temperature effects (Potter et al., **1981).**

In this paper we deal exclusively with the chemical water-rock interaction of a high salinity brine and sandstone containing the mineral anhydrite. Anhydrite has been found in some hydrogeothermal reservoirs in NE-Germany which have been investigated with respect to their geothermal potential. In these aquifers anhydrite cementation by diagenetic processes was the reason for a substantial reduction of permeability.

Reservoir fluids are often brines which are, in respect to particular mineral phases, in equilibrium or even close to saturation for the given formation temperature. In the north German sedimentary basin, this is the case for earth alkaline sulfates and carbonates. When cool water is reinjected into the hot reservoir the equilibrium between the injected water and the reactive minerals is disturbed. This may cause temperature induced dissolution or precipitation. To predict the permeability development of these aquifers one needs to understand the complex interaction of the involved processes -flow, heat transfer, transport of dissolved species, and chemical reactions - over the entire period of operation, which can be analyzed by numerical simulation only. Presently available numerical models (e.g. Cheng

and Yeh, 1998; Ondrak and Moller, 1999; Sandford and Konikow, 1989) do not meet all of the requirements of a suitable numerical code for two reasons: 1. The theoretical approaches on which their chemical model components are based do not describe correctly the situation at high salinities and temperatures observed in the geothermal brines. 2. The permeability-porosity-relation applied in these models has been derived from a pore space geometry which is too simple for the most real sandstones. Laboratory measurements of core samples show a large degree of variation in the sensitivity of permeability to porosity changes (Pape at al., 1999). Therefore, a new relationship between porosity and permeability and a new chemical reaction model were implemented in the numerical code SHEMAT (Clauser and Villinger, 1990). Due to the fact that the injectivity is most sensitive to formation damage in the near vicinity of the injection well (± 1-10 m, Boisdet et al., 1989), this new simulation tool has been applied for a numerical case study of such a well. The objective of the present study was to concentrate on mineral reaction processes and resulting changes of well properties in a limited area around the well.

Chemical reactions taking place in a production aquifer are strongly coupled to species transport as well as to the development of temperature in the formation. For a better understanding of these complex interactions, firstly the fluid-flow regime is described, secondly the temperature effect on the fluid-flow properties is investigated, and finally results are presented showing the anhydrite dissolution and precipitation reactions dependent on the injection temperature. Reservoir properties of a typical aquifer suitable for geothermal utilization are assumed.

2. NUMERICAL MODEL AND CASE STUDY

2.1 Model Components and Numerical Methods

In the simulation code SHEMAT the partial differential equations for flow, heat transfer and multi-component transport are solved numerically by a finite difference approximation. A pure ***upwind scheme,*** the ***Il'in-flux-blending scheme*** (Clauser and Kiesner, 1987), and the ***Smolarkiewicz method*** (Smolarkiewicz, 1983) are implemented for solving the equations for heat and species transport.

The chemical reaction model is a modification of the geochemical simulation code, PHRQPITZ (Plummer ***et al.,*** 1988) and calculates the precipitated or dissolved amount of mineral species for high temperature and salinity. It permits calculations of geochemical reactions in brines and other highly concentrated electrolyte solutions using the Pitzer virial coefficient approach for the correction of activity coefficients. Reaction-modeling capabilities include the calculation of aqueous speciation and the mineral-saturation index as well as mineral solubility. A data base valid for temperatures from 0 to 150 °C of Pitzer interaction parameters is provided for the system Na-K-Mg-Ca-H-Cl-SO,-OH-(HCO,-CO,-CO,)-H_2O. The Pitzer treatment of the aqueous model is largely based on the equations presented by Harvie ***et al.*** (1984), and the data of Greenberg and Moller (1989). Data for the incorporated carbonic acid system (set in parentheses in the list above) are valid for temperatures from 0 to 90°C according to He and Morse (1993). PHRQPITZ was developed by Plummer et al. (1988) incorporating the Pitzer virial coefficient approach (Pitzer, 1973). We extended the PHRQPITZ code to include the calculation of temperature dependent Pitzer coefficients.

All the processes involved, i.e. flow, heat transfer, multi-component transport, and geochemical reactions, are coupled (1) via the dependence of the material and thermodynamic properties on temperature, pressure and species concentrations, and (2) by solving simultaneously the flow, transport, and reaction equations for these quantities. The first way of coupling accounts for the:

- dependence of fluid properties (viscosity, density, heat capacity, thermal conductivity, compressibility) on temperature;
- dependence of fluid density on species concentrations (i.e. density driven flow is possible);
- dependence of rock thermal conductivity on temperature;
- dependence of the chemical equilibrium on temperature and species concentration;
- changes in porosity due to the precipitation and dissolution of minerals;
- fractal relationship between permeability and porosity changes.

The second way of coupling refers to the fact that chemical reactions act as a source or sink in respect to the transport of dissolved species. In our model this is approximated at each time step by subsequently calculating the transport of dissolved species and then the change in their concentrations due to mineral reactions between the reservoir rock and the fluid.

The relationship between permeability and porosity, implemented in the numerical code, is based on the assumption that the shape of the internal surface of rock pores follows a rule of self-similarity. Thus the theory of fractals can be applied. The fractal relationship between permeability k and porosity ϕ was expressed by Pape et al. (1999) as a general three-term power series in porosity:

$$k = A\,\phi + B\,\phi^{expl} + C\,(10\phi)^{exp2} \qquad (1)$$

where the exponents expl and exp2 depend on the fractal dimension of the internal surface of the

pore space. The coefficients A, B, and C, in turn, need to be calibrated for each type of sedimentary basin or pore space modification, i.e. porosity change, due to chemical reactions. Equation 1 reflects the fact that in different porosity regions different processes are responsible for porosity and permeability changes. In SHEMAT this is approximated by Equation 2 and the possibility for the modeler to prescribe different exponents for three porosity intervals. k_0, ϕ_0 denote the initial values containing the same information like the coefficients in Equation 1:

$$k = k_0 (\phi / \phi_0)^{exp} . \qquad (2)$$

The single modules of the numerical model were tested against different standard benchmarks and literature data in order to verify that the various implemented components work correctly and that the code yields results of sufficient quality. The coupling aspects were validated by a successful simulation of the permeability evolution observed during a core flooding laboratory experiment under aquifer conditions. Permeability changes in this experiment where due to internal anhydrite dissolution, transport, and subsequent precipitation (Bartels et al., in prep.).

2.2 Numerical Case Study

The investigated area measures 51*51 m with a layer thickness of 30 m discretisized by an equidistant grid of 1 m^2 node distance. This is big enough to exclude boundary effects in the time period considered. For the two dimensional simulations we chose an imaginary formation which reflects a typical production aquifer in Germany located in 1500 m depth with the appropriate properties (Table 1).

Table 1: Formation properties (isotropic)

Property	Value	Dimension
Anhydrite	0.8	[Weight %]
Porosity	0.15	[-]
Permeability	$0.5*10^{-12}$	[m^2]
Thermal Capacity	0.7	[J/kgK]
Therm. Conductivity	2.5	[W/mK]
Temperature	100	[°C]
Fractal Exponents	1/3/4.85/7	

A sensitivity analysis of the permeability-porosity relationship has been done by simulations carried out with varying exponents related to fractal dimension. Equation 2 applied with an exponent of 1.0 describes permeability changes of average sandstones in the porosity range between 0-1 %. The exponent 3.0 is often used, when no detailed information of the material is available. It is typical for a matrix composed of grains with smooth surfaces. This can be assumed only for clean quartz cemented sandstones (e.g. Fontainebleau sandstone). The exponent 4.85 was obtained from a data set from petrophysical investigations of a sandstone with anhydrite cement, thus we use it to calculate permeability changes caused by anhydrite dissolution and precipitation. In addition the simulations has been repeated with an exponent of 7.0 in which case porosity changes due to chemical reactions cause larger permeability changes compared to smaller exponents.

A dispersion length of 0.5 m is used for transport and the injection well is assumed to be fully penetrated. The injected brine is a solution of 1.7 mol/L sodium chloride with a pH of 7.

3. RESULTS

3.1 Isothermal Flow

The catchment area of the injection well is assumed to be homogeneous and isotropic (Table 1). The aquifer is set to be impermeable at the top and the bottom and to have constant hydraulic head at all four sides. The boundary head value is fixed to coincide with an aquifer depth of 1500 m. The injection well is located in the center of the model area with an injection rate of 50 m^3/h.

Simulations yield that the fluid flow in the investigated area remains unchanged after an injection time of 10 hours. The flow velocities are varying between 7.27 m/day in the near vicinity of the well and 0.33 m/day at the edges of the investigation catchment. After 4 days the front of a tracer, injected for diagnostic reasons, reaches the edges of the investigation area. Therefore, in the following the simulation time is limited to this period.

3.2 Non Isothermal Flow

The temporal development of the hydraulic head is shown in Figure 1 for the first four days at an observation point located 2.5 m from the well. The head increases even in the second half of the period when temperature remains constant. In comparison with the tracer the temperature front, propagating from the injection well, runs behind the tracer front (Fig. 1).

For a more detailed examination of the temperature dependency of the hydraulic head, simulations have been run with varying injection temperatures between 20°C and 100°C. In Figure 2 the hydraulic head, after four days of simulation, significantly depends on the injection temperature. The lower the temperature, the higher the hydraulic head required to maintain a fixed injection rate. The hydraulic head at the well, risen from the initial value of 1500 m to 1560 m at 20°C, corresponds with an excess pressure of 0.6 MPa.

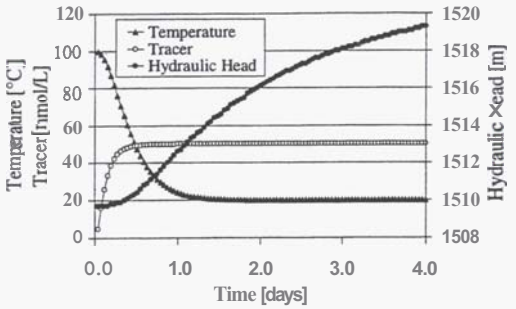

Figure 1: Hydraulic head, temperature and tracer concentration versus time at the monitoring point located 2.5 m from the well.

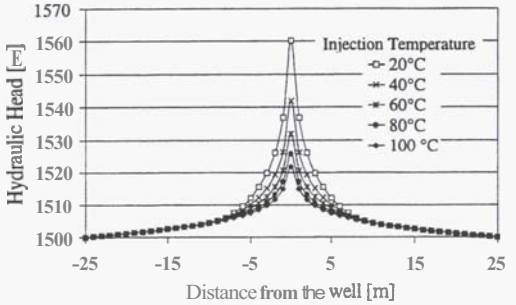

Figure 2: Hydraulic head versus distance from the well after four days of simulation.

3.3 Chemical Reactions

The reservoir sandstone is assumed to be cemented with 0.8 weight % anhydrite, which reacts with the injected water depending on the temperature conditions. This amount corresponds to 8.16 g anhydrite per kg of rock material, which is used as initial value. The mineral is homogeneously distributed over the entire area of simulation. The temporal development of anhydrite, temperature, and calcium concentration, monitored 2.5 m from the well, is shown in Figure 3.

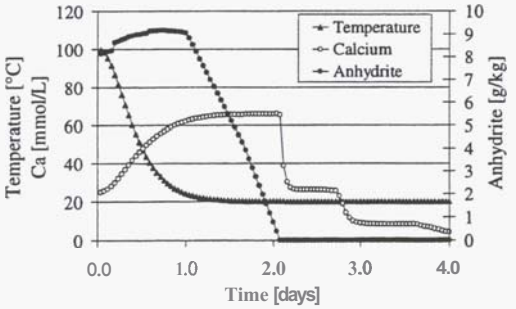

Figure 3: Temperature, amount of anhydrite, and calcium concentration versus time 2.5 m from the well.

The amount of anhydrite at this distance increases during the first day. From then on it reduces until it reaches a value of zero after about two days. The temperature decreases from 100 to 20°C during the first 1.5 days. The calcium concentration of the water in the observed cell rises from 25 to 66 mmol/L during the first two days. At the moment the amount of anhydrite has decreased to zero, the calcium concentration sharply diminishes to 25 mmol/L. Two further steep depletions of calcium occur after about 2.75 and 3.75 days.

Figure4 depicts the spatial distribution of anhydrite after four days of simulation. The amount of anhydrite is reduced to zero in a cylinder with a radius of about 3 m around the well. In a distance of about 5 meters an annulus of nearly 5 meters width can be seen which is enriched with anhydrite. The maximum enrichment of the mineral is 10.7 g/kg risen from the initial value of 8.16 g/kg.

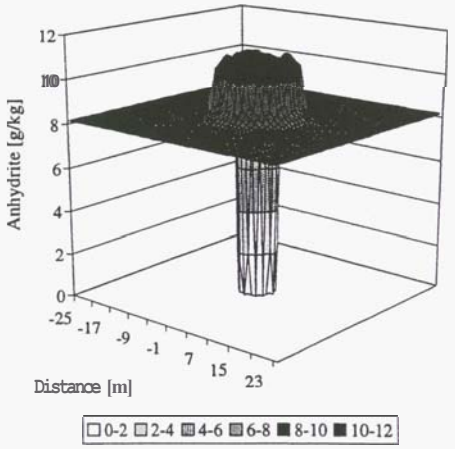

Figure 4: Anhydrite distribution after a time period of 4 days.

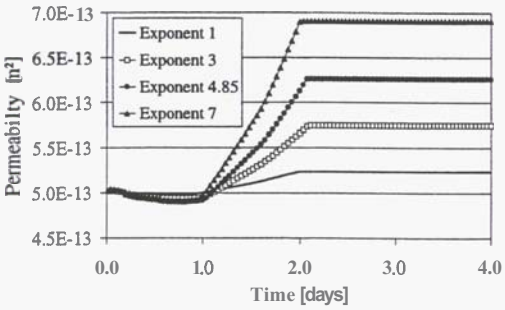

Figure 5: Permeability versus time 2.5 m from the well for varying exponents related to different fractal dimensions of the permeability-porosity relationship.

In Figure 5 the temporal permeability changes are shown in dependency on the applied "fractal" exponent (compare Eq. 2). Simulations have been carried out with exponents of 1, 3, 4.85, and 7. The permeability decreases slightly during the first day of simulation. Between the first and second day the permeability increases and depends on the exponent. In comparison with Figure 3 it can be seen that the permeability evolution reflects the temporal changes of the anhydrite amount.

In Table 2 the resulting hydraulic heads at the injection well are shown after the simulation

period of four days. The injectivity of the formation layer is increased compared to the non-isothermal case of reinjection in Section 3.2. The higher the exponent for the permeability-porosity relationship, the lower the hydraulic head.

Table 2: Resulting hydraulic heads at the well after four days of simulation.

Case	Hydraulic Head [m]
no Chemical reaction	1560
Exponent 1.0	1559
Exponent 3.0	1556

4. DISCUSSION

This case study has investigated the evolution of the hydraulic conductivity in the formation layer and the hydraulic head at the well under the guideline of constant reinjection rates. The propagation of the temperature front spreading is much slower than the propagation of the tracer front (Figure 1) due to the fact, that the water has to cool the rock material. In this term the front velocity depends on the thermal capacity of the formation and the flow velocity of the water (Table 1). The excess pressure necessary for the reinjection strongly depends on the reinjection temperature (Figure 2). With increasing temperature the viscosity η of the water decreases and the hydraulic conductivity k_f of the formation layer increases, which can be understood via its definition:

$$k_f = (k * \rho * g) / \eta , \qquad (3)$$

with the density of water ρ, and the acceleration of gravity g. This is the reason why the hydraulic head does not reach a stationary state during the simulation period (Figure 1). The area already filled with cool water is increasing with time and with it the hydraulic conductivity of the whole aquifer is getting continuously smaller.

Temperature conditions during the injection process control the chemical reactions in the vicinity of the well. We have to be aware of the fact that anhydrite ($CaSO_4$) is more soluble in cold water than in hot water. Thus, in Figure 3 the calcium concentration increases with decreasing temperature. The equilibrium concentration of about 25 mmol/L at 100°C grows during the first 1.5 days to 66 mmol/L at 20°C. After two days anhydrite is totally dissolved and the calcium concentration rapidly decreases. The two further rapid Ca depletions observed have to be explained by the numerics. Near the injection well the rectangular discretisation is too coarse compared to the curvature of the temperature front. Diffusion and dispersion from neighbouring nodes lead to a non-zero calcium concentration even if anhydrite is completely dissolved at this node. The second and third decreases mark the moments when anhydrite disappears at the neighbouring nodes. The depletions are comparatively rapid because we assume no kinetic hindrance of the dissolution and no reduction of the reactive mineral surface.

The injection of 20°C cold water in an aquifer with a formation temperature of 100°C causes dissolution of anhydrite at the injection well (Figure 4), and transport of dissolved anhydrite through the aquifer. The transport process is faster than the spreading of the lower temperature into the aquifer (Figure 1). Therefore, water which is equilibrated at 20°C with higher amounts of Ca and SO_4 reaches the temperature front from behind. At higher temperatures lower amounts of $CaSO_4$ are soluble in the brine. Consequently, anhydrite has to precipitate again because the temperature increases (Fig. 4). This process is accompanied by a reduction of permeability. Finally the anhydrite is dissolved again as the cooling front propagates further. As shown in Figure5 the permeability depends on the actual porosity-permeability relationship. The greater the applied exponent of the fractal dimension, the more sensible is the permeability change due to anhydrite dissolution or precipitation. The increase of the permeability remains zero when the mineral is totally dissolved. As a result of the anhydrite dissolution around the injection well, the injectivity of the layer grows compared to the non reactive case of flow. This is shown by the resulting hydraulic heads at the well (Table 1). In the period considered, the negative effect of the cold water on the injectivity is partially compensated by the relocation of anhydrite in *the* formation. Consequently the influence of mineral dissolution around the well predominates the precipitation at the temperature front. Remarkably great amounts of anhydrite are dissolved and removed from the near vicinity of the well in a relatively short period of time.

5. CONCLUSION

The presented simulations of an idealized injection well belonging to the geothermal doublet installation are referring to a short time scale (first days of heat production) and the near vicinity of the borehole (25 m in radius). In this special case the fluid-flow development was studied dependent on temperature as well as on chemical processes.

The temperature of the reinjected water exerts a great influence on the hydraulic conductivity of the aquifer and thus on the pressure development at the well. The lower the temperature the lower the injectivity of the formation layer. A constant pressure distribution can not be reached in the layer, because the amount of injected cool water is continuously increasing.

The dissolution of anhydrite in the area around the well, induced by temperature changes, increases the permeability, whereas the precipita-

tion of anhydrite at the temperature front reduces it. Relatively large mineral amounts are relocated in time under realistic conditions of a geothermal aquifer. It can be concluded that the negative effect of the temperature on the injectivity is partially compensated by the anhydrite reactions, because the permeability increase predominates the decrease.

Numerical simulation of the complex behaviour of a utilized hydro-geothermal reservoir leads to reliable results only if the processes solved are fully coupled. SHEMAT is a comprehensive tool which meets the requirement and is suitable to carry out substantial parameter studies on geothermally aquifers.

6. ACKNOWLEDGMENTS

The research reported in this paper was supported by the German Federal Ministry for Education, Science, Research, and Technology (BMBF) under grant 032 69 95. We would like to thank Heinke Stöfen for extensive assistance in performance and analysis of the numerical simulations.

7. REFERENCES

Bartels, J., Kuhn, M., Pape, H, and Clauser, C. (in prep.). Simulation of a core flooding experiment. ***Geophysical Research Letters.***

Boisdet, A., Cautru, J.P., Czernichowski-Lauriol, I., Foucher, J.C., Fouillac, C., Honnegger, J.L., and Martin J.C. (1989). Experiments on reinjection of geothermal brines in the deep Triassic sandstones. ***European Geothermal update, Proceedings of the 4th International Seminar on the results of EC Geothemul Energy,*** Florence, 27-30 April 1989, pp. 419-428.

Clauser, C. and Kiesner, S. (1987). A Conservative, Unconditionally Stable, Second-Order Three Point Differencing Scheme for the Diffusion Convection Equation. ***Geophys. J. R. Astr. Soc.,*** Vol. 91, pp. 557-568.

Clauser, C. and Villinger, H. (1990). Analysis of Conductive and Convective Heat Transfer in a Sedimentary Basin, Demonstrated for the Rheingraben. ***Geophys. J. Int.,*** Vol. 100(3), pp. 393-414.

Cheng, H.-P. and Yeh, G.-T., (1998). Development and demonstrative application of a 3-D numerical model of subsurface flow, heat transfer, and reactive transport: 3DHYDROGEOCHEM. J. *Contam. Hydrol.,* Vol 34, pp. 47-83.

Greenberg, J.P. and Moller, N. (1989). The prediction of mineral solubilities in natural waters: A chemical equilibrium model for the Na-K-Ca-Cl-SO4-H2O system to high concentration from 0 to 250 "C, ***Geochim. Cosmochim. Acta,*** Vol. ***53,*** pp. 2503-2518.

Harvie, C. E., Moller, N., and Weare, J. H. (1984). The prediction of mineral solubilities in natural waters: The Na-K-Mg-Ca-H-Cl-SO4-OH-HCO3-CO3-CO2-H2O system to high ionic strengths at 25 "C. ***Geochim. Cosmochim. Acta,*** Vol. 48, pp. 723-751.

He, S. and Morse, J.W. (1993). The carbonic acid system and calcite solubility in aqueous Na-K-Ca-Mg-Cl-SO4 solutions from 0-90 "C. ***Geochim. Cosmochim. Acta,*** Vol. 57, pp. 3533-3554.

Kuhn, M., Vernoux, J.-F., Isenbeck-Schroter, M., Kellner, T., and Schulz, H.D. (1998): On-site experimental simulation of brine injection into a clastic reservoir as applied to geothermal exploitation in Germany, ***Applied Geochemistry,*** Vol. 13(4), pp. 477-490.

Ondrak, R. and Moller, P. (1999). Modeling coupled heat and mass transport applied to the hydrothermal system of the Upper Harz Mountains (Germany). ***Chem. Geol.,*** Vol. 155, pp. 171-185.

Pape, H., Clauser, C., and Iffland, J. (1999). Permeability prediction based on fractal pore-space geometry. ***Geophysics,*** Vol. 64(6).

Pitzer, K. S. (1973). Thermodynamics of electrolytes. 1. Theoretical basis and general equations. ***J. Physical Chemistry,*** Vol. 77, pp. 268-277.

Plummer, L.N., Parkhurst, D.L., Fleming, G.W., and Dunkle, S.A. (1988). ***A computer program incorporating Pitzer's equations for calculation of geochemical reactions in brines.*** U.S. Geological Survey Water-Resources Investigations Report 88-4153, 310 p.

Potter, J.M., Dibble, W.E., and Nur, A. (1981): Effects of temperature and solution composition on the permeability of St. Peters sandstone-Role of iron (III); Journal of ***Petroleum Technology 33*** (5), pp. 905-907.

Sandford, W. E. and Konikow, L. F. (1989). Simulation of Calcite Dissolution and Porosity Changes in Saltwater Mixing Zones in Coastal Aquifers. ***Water Resour. Res.,*** Vol. 25(4), pp. 655-667.

Smolarkiewicz, P. K. (1983). A Simple Positive Definite Advection Scheme with Small Implicit Diffusion, ***Monthly Weather Rev.,*** Vol. 111, pp. 479-486.

Vernoux J.F. & Ochi J. (1994). Aspects relative to the release and deposition of fines and their influence on the injectivity decrease of a clastic reservoir. ***Geothermics 94 in Europe, Int. Symp.*** held in Orléans, France, 8-9 Feb., pp. 291-302.